ADAPTIVE BACKSCATTER COMMUNICATION APPROACH FOR NEXT-GENERATION BIOTELEMETRY APPLICATIONS

A Dissertation
Presented to
The Academic Faculty

By

Bindu Madhavi Kasina

In Partial Fulfillment
of the Requirements for the Degree
Master of Science in the
School of Engineering
Electrical and Computer Engineering

Georgia Institute of Technology

May 2024

ADAPTIVE BACKSCATTER COMMUNICATION APPROACH FOR NEXT-GENERATION BIOTELEMETRY APPLICATIONS

Thesis committee:

Dr. Seun Sangodoyin
Electrical and Computer Engineering
Georgia Institute of Technology

Dr. Matthieu Bloch
Electrical and Computer Engineering
Georgia Institute of Technology

Dr. Morris Cohen
Electrical and Computer Engineering
Georgia Institute of Technology

Date approved: April 26, 2024

The universe is full of magical things patiently waiting for our wits to grow sharper.

Eden Phillpotts

To my family, my partner and my friends.

ACKNOWLEDGMENTS

I take this opportunity to express my profound gratitude and deep regards to my supervisor, Dr. Seun Sangodoyin for his exemplary guidance, monitoring and constant encouragement throughout the course of this thesis. I thank him for taking me under his assistance and for providing his valuable insight during the course of my work. I would like to thank all of my labmates at BioWiNS who provided all the technical support and guidance throughout my time at the lab. I would also like to thank all the professors who have taught me during these past years and empowered me with sound knowledge and understanding required in this project.

I am also grateful to my parents and my friends who have always encouraged and supported me throughout this journey.

TABLE OF CONTENTS

LIST OF TABLES

LIST OF FIGURES

RFID Radio Frequency Identification

LFSR Linear Feedback Shift Register

FPGA Field Programmable Gate Array

RCS Radar Cross Section

RF Radio Frequency

ASIC Application Specific Integrated Circuit

ISM Industrial, Scientific, Medical

CMOS Complementary Metal Oxide Semiconductor

NMOS N-type Metal Oxide Semiconductor

PMOS P-type Metal Oxide Semiconductor

GPIO General Purpose Input Output

POC Proof of Concept

SAR Specific Absorption Rate

UWB Ultra Wide Band

DFF D-flip flop

SUMMARY

This thesis presents the design and implementation of a Proof of Concept (POC) system that adaptively distributes logic gate resources of an Application Specific Integrated Circuit (ASIC) between RFID backscattering and sensor data processing. Building on research previously published in [1] and [2], this work is an extension for the application of digital logic in RFID backscattering systems. The system utilizes the electronic switching capabilities of CMOS transistors within logic gates to create impedance variations between high and low states, effectively altering the Radar Cross Section (RCS) and thereby modulating the backscattered field.

The enhancement detailed in this thesis is the adaptive distribution of logic gate resources based on received signal power at the reader. This capability was not developed in prior systems where the number of logic gate resources used for backscattering was manually set, which can be constraining in fabricated ASICs. A POC system is described in our work, where the reader classifies the received power as low or sufficient. If the received power is low, this information can be encoded into the carrier wave. This carrier wave is incident on the tag, where the tag performs two important tasks: 1) The control circuit decodes the control input from the carrier wave (This part is not in the scope of this Thesis.). 2) The FPGA receives this input and adaptively adjusts the amount of logic gate resources. In addition, the signal incident on the tag is modulated via backscattering from the FPGA's chip. Hence, the FPGA's chip is also responsible for the backscattering. **The primary focus of this work is to enhance the received backscattered signal power by dynamically modifying the amount of logic gate resources on the FPGA based on a given control input.** We detail how information received at the FPGA is utilized to make these adaptive adjustments. We also present the algorithm used to program the FPGA to enable this functionality.

The practical implications of our work are demonstrated through successful measure-

ments, which indicate that higher logic gate utilization correlates directly with increased received power. Our results show up to a 7dB improvement in received power when logic gate utilization of the FPGA is increased from 30% to 100%. The choice of 30% logic gate utilization was arbitrary, and it should be noted that utilizing less than 30% of the logic gates can also effectively yield a backscattered signal. We have also provided results showing that the system adaptively changes the logic gate utilization without the need for reprogramming the FPGA, using internal and external control logic to adjust the logic gate resources dynamically. To prevent any potential interference from the General Purpose Input Output (GPIO) pins which could act as radiators and obscure the backscattered signal, these pins are configured as high impedance nodes. This ensures that the signal power received at the reader is exclusively through backscattering.

In summary, this thesis aims to develop a fully self-sufficient RFID system that facilitates real-time adjustments to backscattering logic gate resources in the ASIC/FPGA based on the strength of the signal received at the reader. The findings from this study provide a solid foundation for the development of an adaptive RFID ASIC system for biotelemetry applications.

CHAPTER 1

INTRODUCTION

The concept of backscattering in RFID systems involves a transmitting device, often referred to as a reader or interrogator, sending out a continuous carrier waveform. This waveform is modulated with information by a device known as the tag, which reflects it back to the reader. The modulation is typically achieved by intentionally creating a mismatch between the input impedance of the tag's antenna and two distinct Radio Frequency (RF) state loads. Traditionally, this mismatch is established using pre-assigned load impedances to vary the tag's reflection coefficient, thereby modulating the incoming waveform. Previous research [2] has demonstrated that such mismatches can also be achieved by utilizing impedance variations in switching circuits, particularly through the use of CMOS inverters that can be configured to two-state RF loads. This approach involves toggling transistor gates between high and low states, which modifies the ASIC's RCS and modulates the backscattered signals effectively.

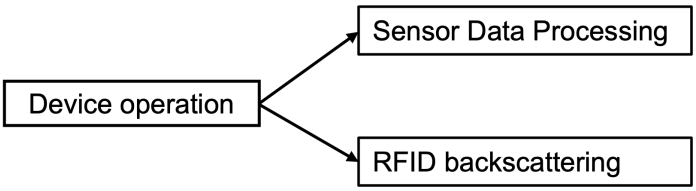

Figure 1.1: Device resource distribution.

A POC system, as referenced in [1], was integrated into the FPGA's internal framework. In this system, flip-flops configured as a Linear Feedback Shift Register (LFSR) were used to toggle between states, achieving the required RF load impedance for signal modulation. The FPGA's resources, including logic gate utilization and power consumption, are divided between two functions: sensor data processing and backscattering as shown in Figure 1.1. The FPGA's chip resource allocation for the purpose of backscattering is a critical aspect

for this system and is measured in terms of logic gate utilization percentages. A higher logic gate utilization for backscattering enhances the received signal power at the reader.

The objective of the proposed research, is to dynamically enhance the quality of backscattered signals from biotelemetry devices. Building on the POC design detailed in [1], this study seeks to adaptively manage the ASIC logic gate resources to optimize effective backscattering for communication. The system is designed to dynamically allocate a higher number of logic gates for backscattering under conditions of low received power, while scaling back resources when the power is sufficient. This adaptive management is expected to significantly improve the quality of the received signal in RFID systems. Since the POC system developed in this work utilizes an FPGA to emulate the design and functionality of an ASIC, we will refer to the FPGA as a *biochip* throughout the remainder of this thesis for ease of discussion.

The contributions of this work are:

1. We provide details on a system that can adaptively control the logic gate resources used in the biochip for backscattering applications.

2. We provide results through measurements conducted, which indicate the flexibility and feasibility of this system.

3. We provide details on the future work aimed at making the system fully automated.

This thesis is organized as follows:

- Chapter 2 provides an overview of RFID backscattering communication, reviews existing literature on its application in biotelemetry devices, and identifies gaps that this research aims to fill.

- Chapter 3 reviews previous work [1] to provide background and continuity.

- Chapter 4 describes the methodology employed in developing and testing the proposed enhancements, along with the advantages offered to the biotelemetry system.

- Chapter 5 presents the conducted measurements and the results obtained.
- Chapter 6 discusses the implications of these findings, concludes with a summary of the research contributions, and discusses directions for future work.

CHAPTER 2
BACKGROUND

2.1 RFID Backscattering communication

RFID communication systems have rapidly become a key part of our daily lives. Some common applications of RFID technology can be seen in supply chain management, asset tracking, data exchange, telemetry, access control, contactless payment methods etc.. These systems, made up of RFID tags and readers, use different power sources, operate at various frequencies, and serve multiple functionalities. The specific properties and rules governing an RFID system affect everything from how much it costs to make, to how well it works, and even its size [3].

An RFID system comprises two main components: an RFID tag and a base station known as the RFID reader. The process of RFID backscatter communication begins with the reader sending out an RF signal. Upon receiving this signal, the RFID tag modulates the carrier signal based on the information stored in its microchip, altering aspects of the signal such as amplitude, frequency, or phase. This modulation encodes the data onto the signal, which is then reflected back to the reader. The reader captures this backscattered signal, demodulates it, and decodes the information, which could include unique IDs, product details, or sensor data. This information enables the reader to take subsequent actions. To facilitate this communication, the input impedance of the tag's antenna is purposefully mismatched with RF state loads, adjusting the tag's reflection coefficient and radar cross-section to modulate the continuous waveform transmitted by the reader. In traditional backscattering, this mismatch is achieved through predetermined load impedances, creating variations in the reflection coefficient that modulate the incoming waveform [2]. Figure 2.1 presents a block diagram showing the operation of a traditional backscatter communication system.

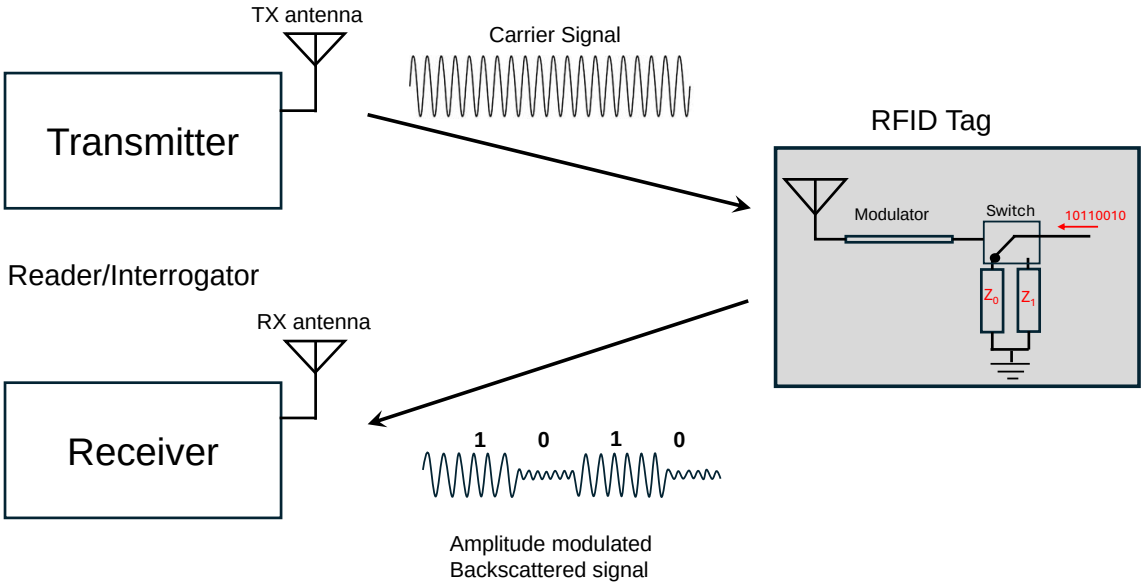

Figure 2.1: Traditional RFID backscattering.

RFID tags are small devices comprising an antenna, a microchip, and an integrated circuit (IC) that stores information unique to the item it's attached to. These tags can be categorized into three main types: active, semi-passive, and passive [4].

1. Active RFID tags: Active RFID tags require an onboard source of energy like a battery, enabling them to communicate over longer distances with readers. The active RFID is similar to a wireless communication system and communicates with readers over a wireless link using radio waves. Hence, active tags can initiate communications with their reader to broadcast information. The communication range of active tags is relatively long, and they may include additional features like large memory or extensibility to add sensors. However, their lifespan and application is limited by their size, weight and cost, as it requires an on chip battery and continuously consumes power even without the presence of a reader.

2. Passive tags: These tags have no onboard power source such as a battery. Instead they derive operational power from the electromagnetic(EM) energy emitted by nearby readers. Their antennas collect this energy, converting it to power the microchip and

enabling the tag to respond. Hence the antenna designed for passive RFID tags needs to collect power from its reader and also reflect or backscatter the outgoing signal. They can be manufactured in very small form factors, and are smaller, lighter, and cheaper but have a shorter communication range compared to battery-operated tags.

3. Semi-Passive tags: Also known as battery assisted passive (BAP) RFID tags, these contain a battery that activates only when the reader detects them. Therefore, their battery lasts longer than active tags and their read range is longer than passive tags. The battery source on semi-passive tags is only used to provide power to the tag circuitry, however these tags do not actively transmit RF signals and cannot initiate the tag-reader communications. They bridge the gap between the limited range of passive tags and the higher cost of active tags, offering a longer read range without actively transmitting RF signals. Their batteries last longer, but they are larger and more expensive than passive tags.

Additionally, RFID tags can be distinguished as chip-based or chip-less. While active and semi-passive tags usually contain chips for enhanced functionality and memory, there's a growing interest in chip-less RFID technology within the passive tag category, aiming to lower costs and expand applicability.

The use of backscatter communication in RFID technology has been explored in various publications, addressing a range of practical applications. [5] explored the use of RFID for asset tracking. [6] introduced a design for a ultra wide band (UWB) RFID tag, while [7] presented a novel active UWB reflector RFID tag equipped with a broadband amplifier, specifically designed to enhance the RCS for applications in wireless sensors. [8] proposed a backscatter system tailored for secure, short-range contactless access control and authentication applications, emphasizing the need for security in backscattering applications. These studies illustrate the ongoing innovations in RFID-based backscatter communication, contributing to the evolution of this technology for different contexts and applications.

2.2 Biotelemetry

Telemetry, a technology that enables data measurements from a distance, plays a critical role in various applications, notably in the testing of moving vehicles like cars, aircraft, and missiles. Biotelemetry, a specialized subset of telemetry, focuses on the measurement of physiological signals. These signals are captured using appropriate transducers, processed, and then transmitted to an external monitoring or control device. This external device can either be attached to the patient's body or placed nearby, with the capability to further communicate with distant medical facilities or physicians through advanced technologies and infrastructure.

The essence of biotelemetry lies in leveraging recent advancements in both wired and wireless communication technologies to meet the increasing demands of the healthcare community. The aim is to harness these advancements to develop a new generation of medical devices with biotelemetry capabilities. Medical devices, useful for preventive, diagnostic, monitoring, or therapeutic functions, support a wide range of medical applications. These devices fall into three categories based on their placement relative to the patient's body: wearable, implantable, and ingestible devices. As example for each of these types of devices is presented in Figure 2.2. Wearable devices can be incorporated into clothing or accessories to monitor various physiological parameters, assist with artificial limbs, and collect and transmit vital signs. They monitor electrical, physical, and physiological parameters in a noninvasive way. Figure 2.2a shows a wearable insulin patch. Using a tiny, flexible cannula, it can deliver rapid-acting insulin under the skin [9]. Implantable devices, surgically placed inside the body, serve purposes like heart rate control and functional electrical stimulation. Figure 2.2b shows an EndoStim implantable pulse generator implant is located in a subcutaneous pocket in the anterior abdominal wall and the bipolar electrodes are implanted in the lower esophageal sphincter muscle. This device is used for electrical stimulation therapy for Gastroesophageal Reflux Disease [10]. Ingestible devices

are swallowed by the patient to monitor gastrointestinal tract activity and drug usage. Most of the invasive (implantable and ingestible) medical devices monitor human-generated metrics like Ph, temperature etc.. Figure 2.2c shows a 3/4 inch, CorTemp Ingestible Core Body Thermometer Pill that wirelessly transmits core body temperature as it travels through the human digestive tract. A sensor within the pill sends a signal that passes harmlessly through the body to the CorTemp Data Recorder outside of the body [11].

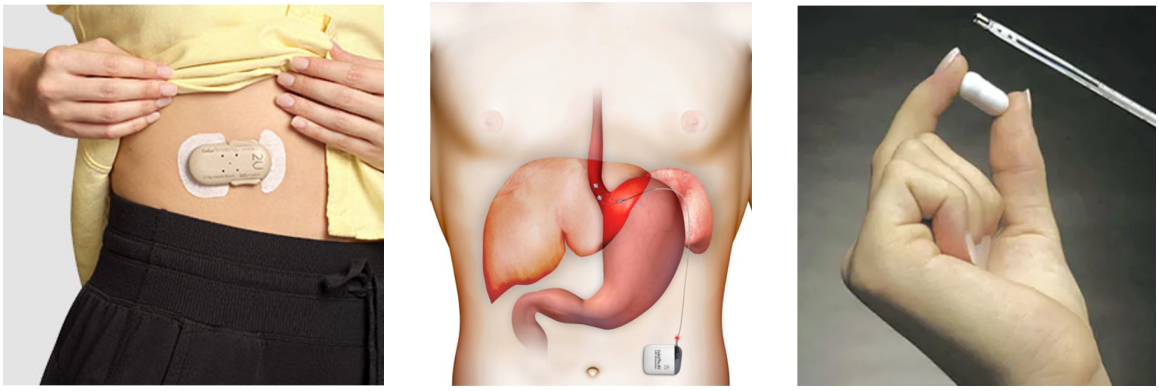

(a) (b) (c)

Figure 2.2: Different types of Biotelemetry (wearable, implantable and ingestible) devices.

Historically, biotelemetry relied heavily on wired connections, which posed limitations in terms of communication range, patient comfort, and activity levels. The shift towards wireless technologies aims to address these challenges, offering accurate physiological signal measurements from patients without restricting their movement. Since the significant development of Internet traffic, digital cellular communication systems, and the advancement of integrated circuits, there has been an increasing amount of research focused on wireless telemetry, thereby driving the medical industry towards the adoption of wireless biotelemetry, a promising and less invasive option [12].

Biomedical devices, whether worn, implanted, or ingested, requires the communication with sensors providing physical, chemical, and biological data for continuous monitoring of the physiological state. This data is then sent to a central device located on or near the patient for further processing, decision-making, emergency notifications, and local storage

for future medical analysis. These devices often incorporate biosensors to gather essential health information, which is transmitted externally for diagnosis via a wireless transmitter. The design of these bio-implants is critical due to their proximity to biological tissues, emphasizing the need for non-intrusiveness, heat generation within safe limits, and high power efficiency for invasive devices to extend their operational lifespan.

Several challenges need to be addressed before designing a wireless biotelemetry system. Since medical devices are used on human beings, with at least a theoretical potential for misuse or harmful side effects, they must first meet the criteria established by government-operated regulations before they can be designated as medical devices and enter the market. Also, demand on radio spectrum for use in wireless biotelemetry systems is currently on the increase. This demand is driven by a rapid increase in the use of medical devices, advancements in wireless communication technologies, and the need to improve quality, reliability, and delivery of health care. This necessitates effective management of the frequently used communication bands like the Medical Implant Communications Systems (MICS) band, the Wireless Medical Telemetry Service (WMTS) bands, the industrial, scientific, and medical (ISM) bands, and the UWB to minimize interference risks [13].

Recent advancements in medical technology have greatly enhanced the capabilities of diagnostic and therapeutic devices, particularly ingestible sensors and devices designed for the gastrointestinal tract. These innovative biosensors are deployed within the body and are capable of performing a broad range of functions. They enable detailed imaging for diagnosing complex medical conditions, allow precise monitoring of internal factors such as temperature [14] and pH levels [15], and facilitate the controlled release of medications directly into the gastrointestinal system [16], [17]. Such technologies not only improve the accuracy of diagnostics and treatments but also hold significant potential to enhance patient care for a variety of widespread gastrointestinal issues. These developments represent a notable step forward in the field of biotelemetry, offering new possibilities for medical intervention and monitoring.

2.3 RFID backscattering for Biotelemetry applications

RFID backscattering technologies are increasingly used in biomedical applications for a variety of functions. These include monitoring vital health parameters, identifying animals and humans, as well as recognizing orthopedic prostheses. Additionally, RFID can assist in patient information registry, services for the handicapped, and laboratory analyses. In implant applications where area and power are limited, passive backscattering technologies are typically adopted. Given the proximity required for these applications, a communication range of less than 10 cm is usually sufficient.

Biomedical implants designed for in-body health monitoring, such as glucose sensors, prioritize compact device size and low power consumption to minimize heat radiation. RFID backscattering does not need an antenna for transmission thereby reducing the device size in comparison with wireless transmission technologies. A glucose sensor implanted under the skin that continuously monitors glucose levels is presented in [18]. In this, the sensor receives power wirelessly from a base station located directly above the implant and transmits data back to the station using backscattered signals. A similar backscatter communication technology has been used for in vivo alcohol monitoring implants in [19].

The physical size of biomedical devices is often constrained by the location of the implant, necessitating smaller device dimensions. As a result, active RFID tags, which tend to be larger due to their battery requirements, are less common. Passive tags, which do not require batteries, are generally preferred. Recent innovations aim to eliminate or reduce the need for batteries in bioimplants through external powering methods or energy harvesting techniques in the gastrointestinal tract. The first implementation of a passive RFID tag with read-only memory for patient monitoring was introduced at [20]. Other works in [21], [22] and [23] use traditional passive RFID tags for backscattering in bioimplants. A multi-antenna approach has added flexibility in controlling the frequency of incident waveforms in [24], although it also increases system complexity.

Bio-compatibility of the materials used in manufacturing implants is crucial to prevent tissue damage. The electromagnetic energy emitted from the reader to the tag must not exceed the maximum allowable specific absorption rate (SAR), as this could lead to a temperature increase in the surrounding tissue. In addition, when considering the deployment of RFID implants, it's important to carefully select the frequency for communication and also account for the attenuation of signals by human tissue. Low Frequency RFID communication (120–145 kHz) experiences minimal attenuation by human tissues, though it has a limited communication range and larger antenna size compared to higher frequencies. High Frequency RFID systems (13.56 MHz) are also relatively unaffected by human tissue and are suitable for communication with multiple implants due to their similar read range to free space propagation. Conversely, Ultra High Frequency RFID devices, allows for higher data rates and more reliable security, but are substantially attenuated by human tissue, resulting in shorter read ranges. Particularly, frequencies at 2.45 GHz and above may pose safety concerns due to absorption of RF signals by the tissues [25].

CHAPTER 3

LEVERAGING ON-CHIP TRANSISTOR SWITCHING FOR RFID BACKSCATTERING IN BIOTELEMETRY APPLICATIONS

In this chapter, we briefly describe the RFID backscattering system implemented in [1]. In traditional backscattering, a mismatch between the impedance associated with a radiating antenna element and predetermined load impedances is required to achieve the backscattering. This principle can also be implemented using digital electronics, specifically through an ASIC consisting of CMOS inverters made from N-type Metal Oxide Semiconductor (NMOS) and P-type Metal Oxide Semiconductor (PMOS) transistors. CMOS inverters have two-state RF loads, and can be effectively used for modulating backscattered signals due to their ability to switch between high and low output states.

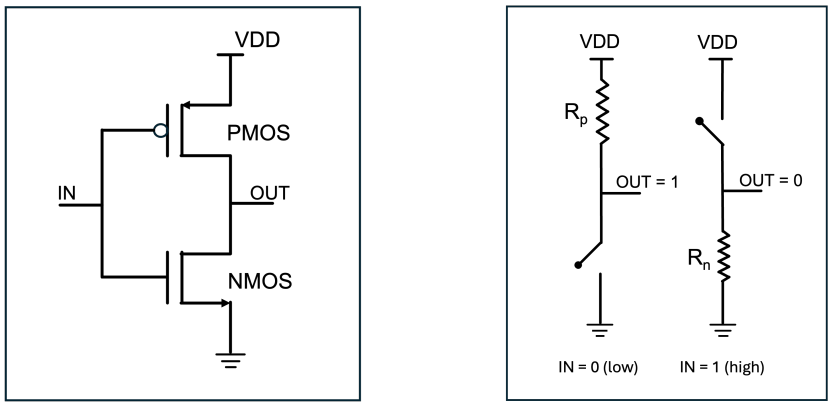

(a) (b)

Figure 3.1: (a) CMOS Inverter. (b) Inverter states at Input low and Input high.

The functionality of a CMOS inverter is as follows: when the input voltage to the inverter is low, the NMOS transistors are turned off, while the PMOS transistors are active. This configuration establishes a direct connection between the output voltage (Vout) and the supply voltage (VDD) through a finite resistance, resulting in a high output state. Conversely, when the input voltage is high, it triggers a low output state as the connection

shifts from the output to the ground, again through a finite resistance. Figure 3.1 shows the schematic of a basic CMOS inverter and the load states of the inverter when the input is either high or low. Using CMOS transistors, digital logic gates such as NOR and NAND are designed. These gates are fundamental in creating complex digital electronic circuits, including registers, which are essential for data storage and can also be connected to other digital components. One of the core components used in registers is the D-flip flop (DFF), which is designed from a combination of NAND gates and inverters as shown in Figure 3.2. The alteration between high and low output states in NAND logic can lead to an impedance variation similar to that seen in antenna terminating impedances in traditional RFID tags. This variation in impedance modifies the RCS of the circuit, facilitating modulation of the incident signal before it is backscattered.

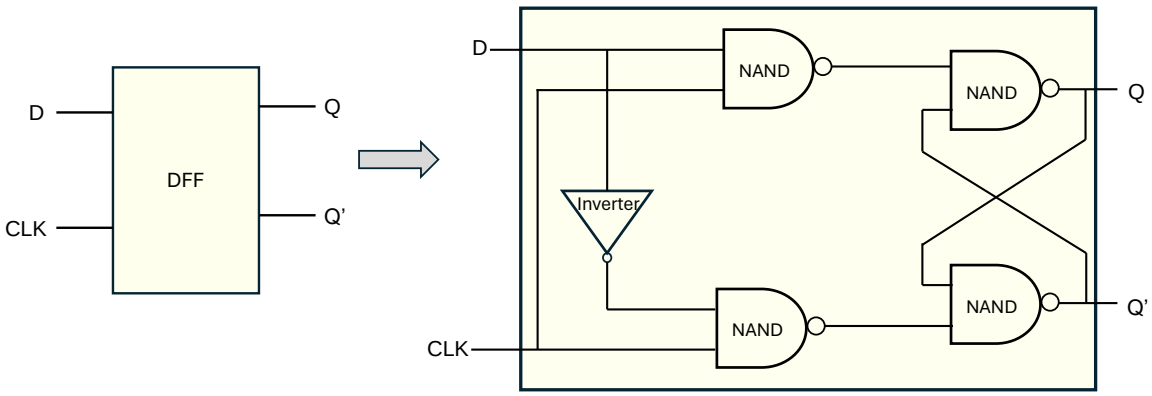

Figure 3.2: D-FlipFlop

To demonstrate the practical application of transistor switching in backscatter communications, an FPGA chip was utilized. Within this chip, a LFSR was configured with continuously connected flip-flops, as shown in Figure 3.3. The output from the LFSR is cyclically fed back into the register using a selected pattern. To modulate the continuous waveform with the carrier frequency (f_c), the flip-flops within the LFSR were programmed to alternate between high and low states at an on-board clock frequency (f_{clock}) rate of 50MHz for half of the cycle, remaining dormant for the other half, thereby establishing a modulation frequency (f_m). The resulting frequencies of the modulated backscattered signal are

consequently written as $f_c \pm f_m$.

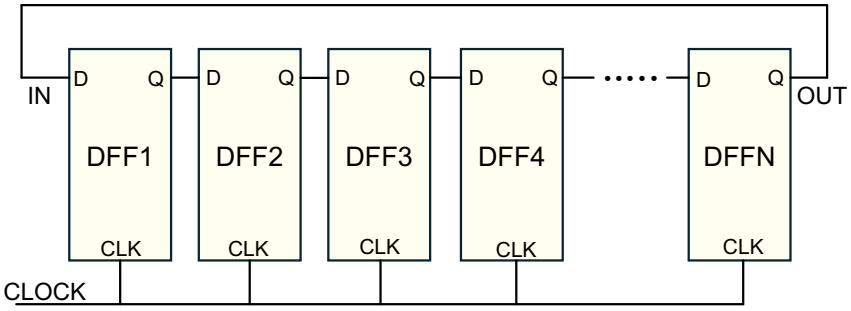

Figure 3.3: Linear Feedback Shift Register

In addition to its backscattering functions, the biochip also handles data processing from incoming biomedical sensors. The biochip's resources, including logic gate utilization and power consumption, are divided between these two functions—sensor data processing and backscattering as shown in Figure 1.1. This efficient allocation allows the biochip to manage both the high demands of sensor data processing and the precise control required for effective backscattering, making it adaptable for modern communications and biomedical applications.

This system presents several key advantages over existing technologies in the field of RFID backscatter communication, particularly in its design simplicity and operational flexibility. Unlike conventional systems that require antennas and extensive redesigns for frequency modulation changes, this system is antenna-less. Also, it offers spectral flexibility by allowing the modulation frequency to be easily adjusted through changes in the switching rate of the flip-flops within the LFSR on the chip. This system also has capability to adjust frequencies without significant design alterations or addition of new components unlike most state-of-the-art works. Moreover, it is capable of transmitting both single and multiple bits simultaneously, a function that state-of-the-art devices typically cannot perform without supplementary hardware. For multi-bit transmission, logic gate utilization is distributed among the bits, activating different LFSRs for each bit to switch at varied modulation frequencies. This system allows for more complex communication tasks to be

executed efficiently.

Successful biotelemetry measurements have been conducted in [1] with this system through biological and phantom tissues. Its antenna-less and front-end-less design makes it not only flexible and versatile but also a significant enhancement over current technologies. The backscattered waveforms produced are capable of penetrating tissues of various compositions and thicknesses, as well as different fluids, maintaining effective power transmission up to distances of 55cm from the tag. Results have also indicated robust signal strength with low Bit Error Rates (BER), alongside the capability to transmit data about varying tissue temperatures measured by a biosensor. This performance highlights the system's potential in advancing RFID backscatter communication for medical and biotelemetry applications.

In the next chapter, we will explore one of the main challenges encountered with this system and provide details on how to enhance its efficiency.

CHAPTER 4

ADAPTIVE LOGIC CONTROL FOR RFID BACKSCATTERING

A POC design of a biosensing and communication system detailed in [1], and briefed in chapter 3, demonstrates an on-chip transistor switching system for RFID backscattering that can be utilized in neural and gastrointestinal biotelemetry. In this chapter, we propose the concept of adaptive logic control for this system introduced in the previous work, aiming to enhance the quality of backscattered signals from biotelemetry devices. This chapter specifically focuses on how to manage the biochip's logic gate resources adaptively to optimize effective backscattering for communication.

As discussed in the previous chapter, this system which is implemented using an FPGA, utilizes an LFSR that is continuously connected through DFFs constructed from CMOS NAND gates. This setup creates the necessary impedance variation, leading to changes in the circuit's RCS, which is crucial for steady communication and efficient data transmission. The FPGA's resource allocation is considered in terms of logic gate utilization percentages, with tasks divided between sensor data processing and backscatter communication. This division is essential as a bioimplant with multiple sensors demands signif-

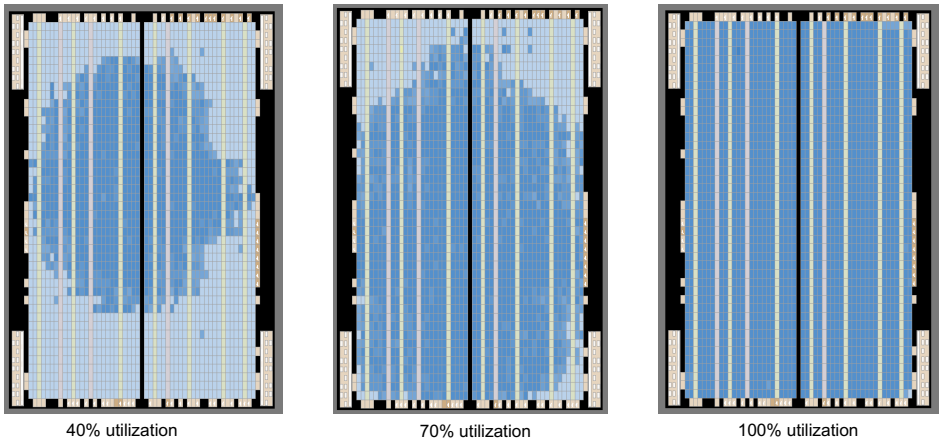

Figure 4.1: On-chip Logic Utilization.

icant on-board data processing resources while also needing resources to backscatter the processed information to the reader. The FPGA's resources are distributed such that the maximum logic gate utilization reaches approximately 100%, corresponding to N=82,000 logic gates dedicated to backscattering. An example of logic gate utilization mapping in an FPGA, modeled through Intel Quartus, is presented in Figure 4.1. The advantage of higher logic gate utilization for backscattering is that, it improves backscattered signal power, flexibility in on-demand assignment of additional resources to auxiliary applications like sensor data processing, and indirect control over the power consumption and thermal profile of the device. This control is critical since excessive heat dissipation could cause irreversible damage to biological tissues.

Measurements conducted in [1] indicated that the received power tends to decrease with a lower percentage of logic gate utilization and an increasing distance between the chip and the reader. By employing more logic gates to control the modulation, there is an increase in the effective active area contributing to signal reflection. Additionally, the use of more logic gates implies that more energy is being modulated, which may be another factor leading to a stronger overall reflected signal. Therefore, selecting an optimal utilization percentage is crucial. However, increased logic gate utilization is expected to raise the power consumption of the chip, consequently leading to higher heat emission from the chip. Results provided for the dependency of power and temperature on logic gate utilization indicated that, the chip could be operated for 37 seconds at 100% logic gate utilization before reaching a 1.5^{o}C increase in temperature, which is the maximum rise the human body can tolerate and any more increase can damage the tissue in the area.

A challenge identified in the referenced study is the need to manually adjust the logic gate utilization to modify the backscattered signal power. As the percentage of logic gate utilization is critical for adjusting the strength of the backscattered signal, an adaptive system has been proposed to more efficiently manage logic gate resource allocation. Figure 4.2 represents the block diagram of the system through which we can address this problem

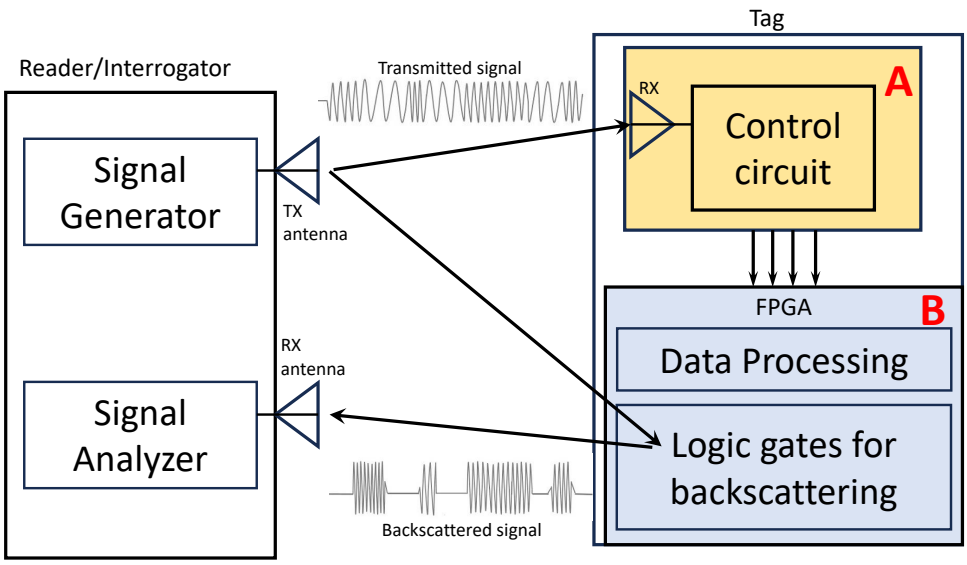

Figure 4.2: System for Biotelemetry with additional circuitry for Integrated power control.

of adaptive logic gate resource management. This system dynamically allocates a higher number of logic gates for backscattering in conditions of low received power, while scaling back resources when the received power is adequate. The adaptive logic gate resource management system is designed to significantly improve the quality of the received signal in RFID systems. Two major challenges are associated with implementing this adaptive system:

1. Communicating the information of received power at the reader to the tag.

2. Allocating resources for backscattering at the tag depending on the received power.

To implement this system, the reader determines the exact amount of logic gate resources the tag can utilize to ensure that the power is sufficient for the reader to accurately decode the transmitted information. This process involves encoding a 3-bit control input into the carrier wave transmitted to the tag. This input specifically directs the percentage of logic gate resources that should be utilized by the tag for improving the backscattered signal strength.

The tag system consists of two main sections: Section A (Control Circuit) and Section B

(FPGA), each implementing different tasks as depicted in Figure 4.2. Upon reception of the carrier wave at the tag, the control circuit (section A) decodes this information and sends it to the FPGA (section B). From this data, the logic gate utilization resources required for optimal backscattered signal strength is determined. The determined percentage of logic gate utilization then dictates how much of the FPGA's resources are dedicated to the LFSR for signal modulation, while the remainder is allocated to processing sensor data. This adaptive approach allows for dynamic resource management, ensuring optimal use of the FPGA's capabilities to enhance communication efficacy and reliability in varying signal conditions. Please note that, although the entire system idea has been discussed, this work primarily focuses on implementing section B of the tag system.

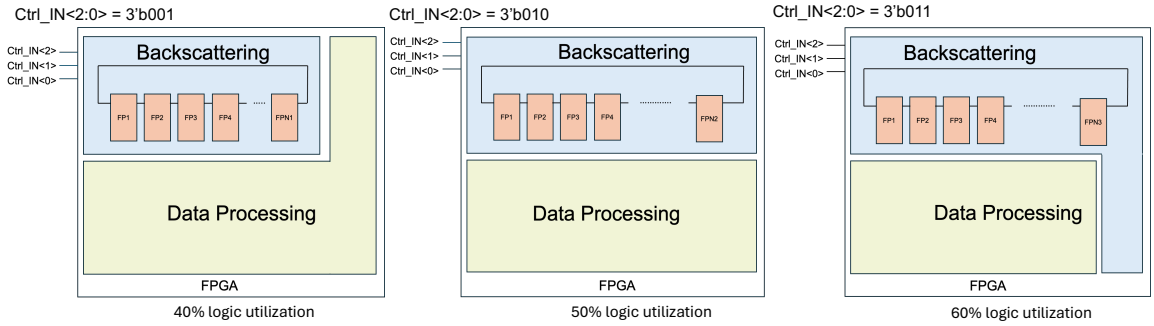

Figure 4.3: Varying Logic Gate Utilization with Control Input.

In this work, we provide external information about the received power, that is, we adaptively alter the resource allocation for the purpose of backscattering given an external control input. As shown in Figure 4.3, a 3-bit external input is used to control the percentage of logic gate resources used. There are 2 major algorithms used to achieve the functionality of logic backscattering at the desired frequency:

Algorithm 1 depicts the generation of the modulation frequency. The main loop is largely controlled by $\mathbb{S}$, which is responsible for generating the modulation frequency by flipping its state at the desired frequency. The $\mathbb{N}$ bit large LFSR denoted by $\mathcal{R}$, switches at the device clk frequency (50MHz) and encodes the data to be transmitted into this modulation frequency. During the operation of the device, when $\mathbb{S}$ is at logic 0, the LFSR is constantly

Algorithm 1: LFSR switching for desired frequency using clock signal

Input: clk; $\mathcal{D}$
// clk → clock signal; $\mathcal{D}$ → current bit being transmitted
Output: $\mathcal{R}[\mathbb{N}-1:0]$
// $\mathcal{R}$ → register; $\mathbb{N}$ → flip-flop (logic gate resource) count
/* Initialization */
$\mathcal{V}$;
// predefined constant to achieve the desired modulation frequency
$count \leftarrow \mathcal{V}$;
$\mathbb{S} \leftarrow 0$; // Switches with the modulation frequency
$\mathcal{R} \leftarrow 0$; // Initial state of the shift register
/* Main Loop */
if *positive edge of clk detected* **then**
    $count \leftarrow count - 1$;
    if $\mathbb{S}$ *and* $\mathcal{D}$ **then**
        $\mathcal{R} \leftarrow\sim (\mathcal{R}[0], \mathcal{R}[\mathbb{N}-1:1])$;// right shift and invert data
    else
        $\mathcal{R} \leftarrow \mathbb{N}'b0$;// assign 0 to all registers
    if $count = 0$ **then**
        $\mathbb{S} \leftarrow\sim \mathbb{S}$;
        $count \leftarrow \mathcal{V}$; // Reset count to predefined parameter

reset. When $\mathbb{S}$ is at logic 1, the loop carries out *shift right* operation on the LFSR depending on the current bit of the incoming data sequence.

Figure 4.4 shows an example waveform generated by this scheme. In this, $\mathbb{S}$ denotes the modulation frequency, and $\mathcal{D}$ indicates the bit currently being transmitted. From this waveform, it's evident that all bits of $\mathcal{R}[\mathbb{N}-1:0]$ switch at the frequency of the clk when both $\mathbb{S}$ and $\mathcal{D}$ are at a logic high. The waveform indicates that, no switching occurs when the transmitted bit is low. This synchronized switching of $\mathcal{R}[\mathbb{N}-1:0]$ at the modulation frequency ensures that data transmission aligns with the frequency set by $\mathbb{S}$. This method guarantees that the data is being transmitted at the modulation frequency generated by $\mathbb{S}$.

Table 4.1 shows the percentage of logic gate utilization and the corresponding number of DFFs used for the LFSR within the DE10 Nano Cyclone V FPGA, given a specific control

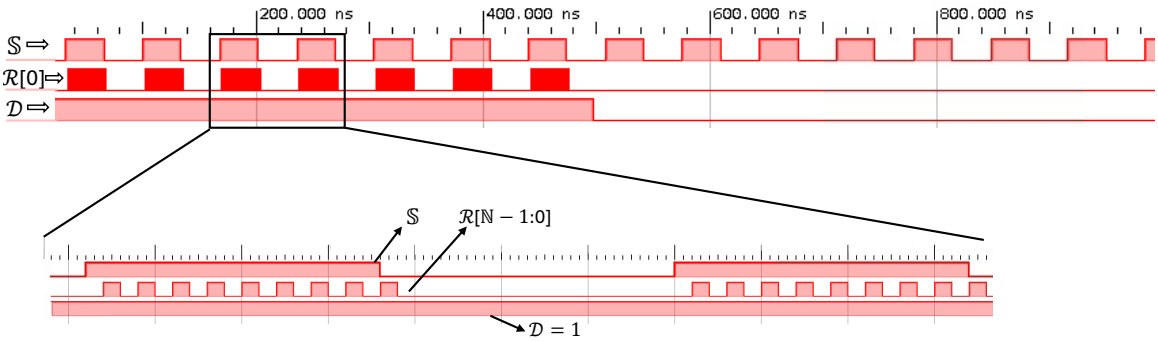

Figure 4.4: Operation waveform for modulating data signal.

Table 4.1: Logic Gate Utilization Reference.

Control Input	**Logic Utilization Percentage**	**No. of Logic Gates**
default	30%	24600
001	40%	32800
010	50%	41000
011	60%	49200
100	70%	57400
101	80%	65600
110	90%	73800
111	100%	82000

input. Further detailed in Algorithm 2 is the process by which the number of logic gates is calculated based on a control input. This adaptive logic gate resource distribution ensures that once the necessary number of logic gate resources ($\mathbb{N}$) is determined, only that quantity is utilized for the switching processes essential for generating the backscattered signal. The remaining logic gate resources are then available for processing sensor data, optimizing the FPGA's capacity for multiple functions. Algorithm 2 is integrated with Algorithm 1 to generate the backscattered signal and also for the simultaneous modulation of the data being transmitted at the desired frequency.

Algorithm 2: Adaptive Logic Gate Resource Distribution

Input: $\mathcal{I}$, $\mathcal{D}$
// $\mathcal{I}$ → decoded bits after demodulation
// $\mathcal{D}$ → current bit being transmitted
Output: $\mathcal{R}[\mathbb{N}-1:0]$
// $\mathcal{R}$ → register; $\mathbb{N}$ → flip-flop (logic gate resource) count
/* Initialization */
$\mathbb{L} = 82000$;
// maximum logic gate resources available
$\mathbb{S} \leftarrow 0$; // Switches with the modulation frequency
$\mathcal{R} \leftarrow 0$; // Initial state of the shift register
/* Inner Loop */
Define guard band bits;
Detect sequence of guard band from $\mathcal{I}$;
Detect control input ($\mathbb{C}$), the 3 bits after the guard band sequence from $\mathcal{I}$;
$\mathbb{N} = (\mathbb{C} + 3'b011) * 0.1 * \mathbb{L}$; // Computed % of logic gate resources to be used.
if $\mathbb{S}$ *and* $\mathcal{D}$ **then**
    $\mathcal{R} \leftarrow\sim (\mathcal{R}[0], \mathcal{R}[\mathbb{N}-1:1])$;// right shift and invert data
    $\mathcal{R}[\mathbb{L}:\mathbb{N}] \leftarrow 0$; // Resources can be used for data processing
else
    $\mathcal{R} \leftarrow \mathbb{N}'$b0;// assign 0 to all registers

In the next section, we present the measurements conducted using this system and provide detailed results.

CHAPTER 5

MEASUREMENTS & RESULTS

A system for this adaptive logic utilization for digital logic backscattering has been designed. Our measurement setup uses an Altera DE10-Nano Cyclone V FPGA chip, functioning as the RFID tag. The maximum of 100% logic gate utilization on the FPGA uses N=83000 flip-flops. Table 4.1 shows the corresponding N for each logic utilization. For the reader, we used two Ultra Wide Band (UWB)(0.7GHz to 8 GHz) horn antennas, ComPower AH-118 model. We generated the carrier wave using a Tektronix AWG7102 Arbitrary Waveform Generator. An Agilent PXA N9030A vector signal analyzer was used to record the received backscattered waveform. A block diagram of the setup is presented in Figure 5.1. The system operates in the 900MHz Industrial, Scientific, Medical (ISM) band, with the carrier frequency set at 900MHz and the modulation frequency at 1.47MHz. We selected these frequencies to comply with the safety standards for in-body transmission, which permits a maximum power of 28dBm for frequencies below 1GHz.

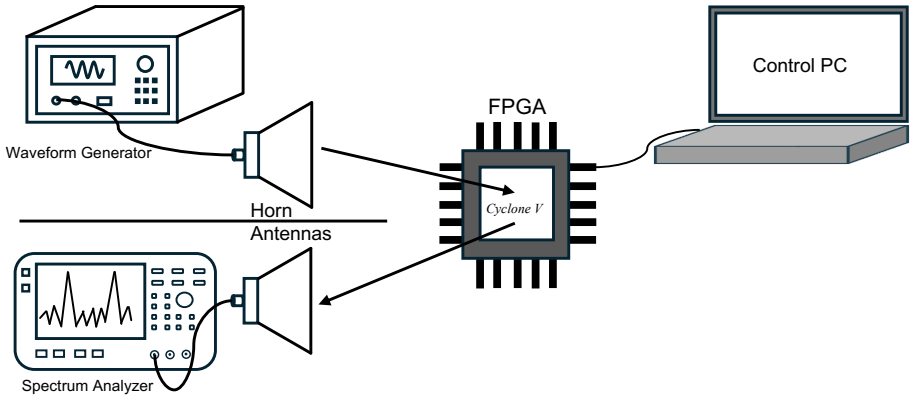

Figure 5.1: Measurement setup block diagram.

In our experimental setup, the GPIO pins, that are commonly used on integrated circuits to facilitate connections with other auxiliary components could act as active radiators. However, to ensure the accuracy of our data, these pins were deactivated during the mea-

surement recordings. This ensures that the signal that we are observing is primarily because of the backscattering from the FPGA chip and not due to the GPIO radiations.

We will present the details about the various experiments conducted to test the functionality of the system in being able to adaptively change the backscattered signal. These measurements were conducted in a 12.5m × 6.2m × 3m laboratory on the 2nd floor of the Technology Enterprise Park Building, outside the campus of Georgia Institute of Technology, Atlanta, GA, USA. The space was equipped with workbenches, chairs, test and measurement devices (such as digital sampling oscilloscopes and network analyzers), and storage cabinets. Figure 5.2 shows the experimental setup used for these experiments.

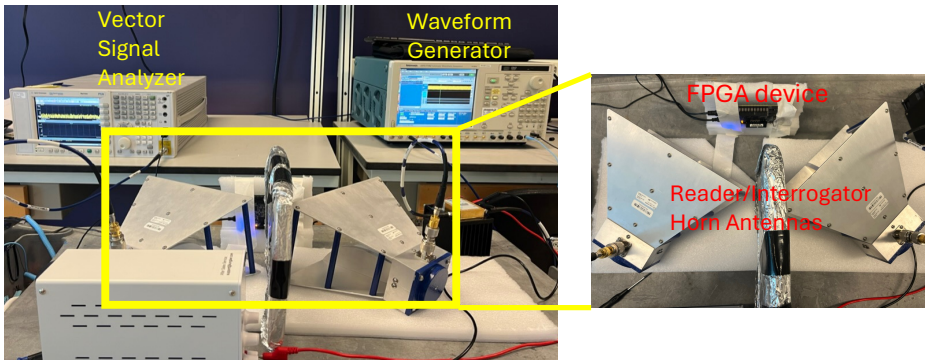

Figure 5.2: Measurement setup.

We placed the FPGA device in front of the antennas and programmed it to operate at 100% logic gate utilization. The LFSR inside the FPGA was programmed to switch at a frequency of 1.47MHz. The waveform generator was setup to transmit a 900MHz carrier wave through the horn antenna.To verify the device's proper operation and that the internal switching occurred at our target frequency of 901.47MHz, we configured one of the GPIO pins to emit the signal. This pin was controlled by a slide switch, which could either enable or disable the transmission. When the switch was off, the pin was set to high impedance, ensuring that any detected communication was solely due to backscattering from the device. After confirming the switching frequency via the GPIO pin, we turned off the slide switch to observe the backscattered signal. Figure 5.3 depicts the signal at 901.4702MHz captured through backscattering from the device at 100% logic gate utilization.

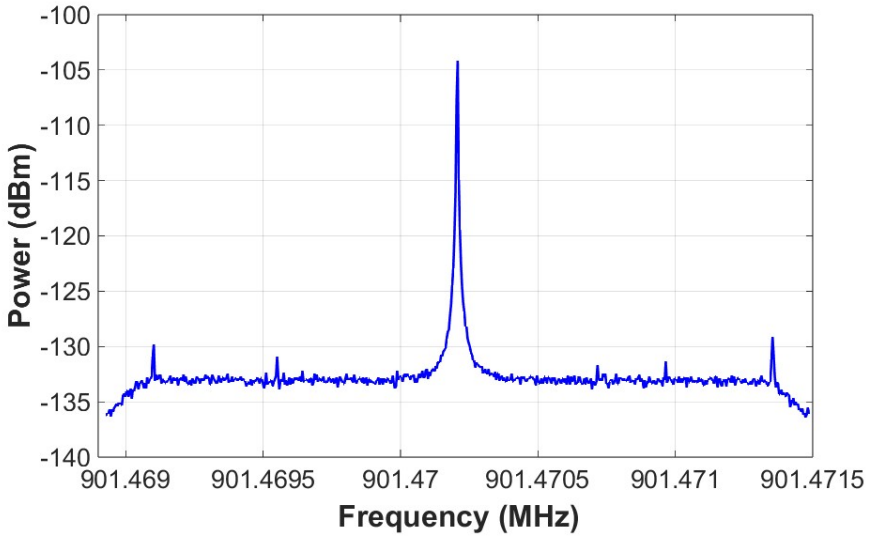

Figure 5.3: Received backscatter signal.

Next, we programmed the FPGA device to operate at various percentages of logic utilization, ranging from 30% to 100% in increments of 10%. This was done to confirm whether increased logic utilization actually enhances the strength of the received power. Figure 5.4

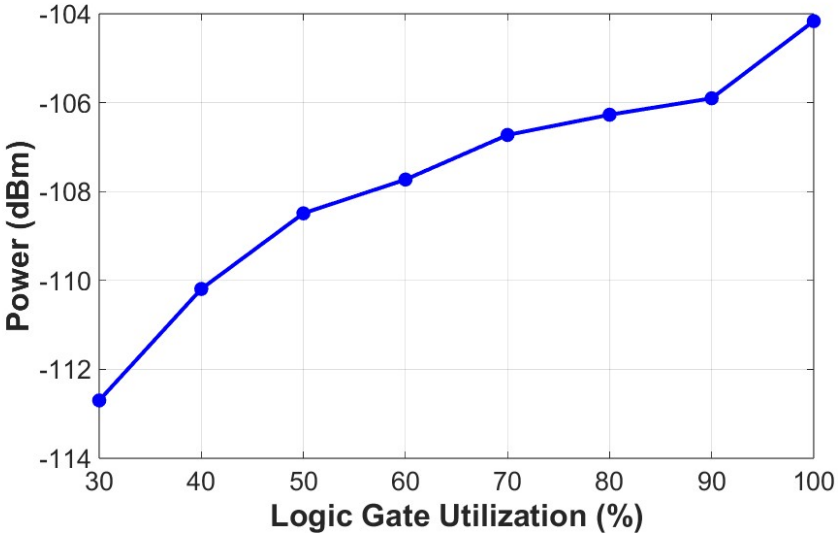

Figure 5.4: Received power with increased logic utilization.

illustrates this, showing an approximate 8dB increase in received signal strength from 30% to 100% utilization.

The FPGA was then programmed to automatically change the logic gate utilization in-

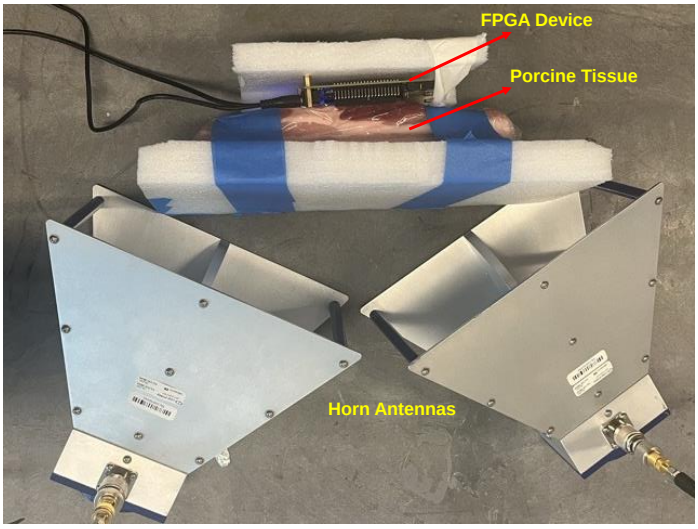

Figure 5.5: Setup with Tissue.

ternally. Initially the logic gate utilization was set at 30% and was programmed to increase the utilization by 10% every minute. We conducted this experiment under two conditions:

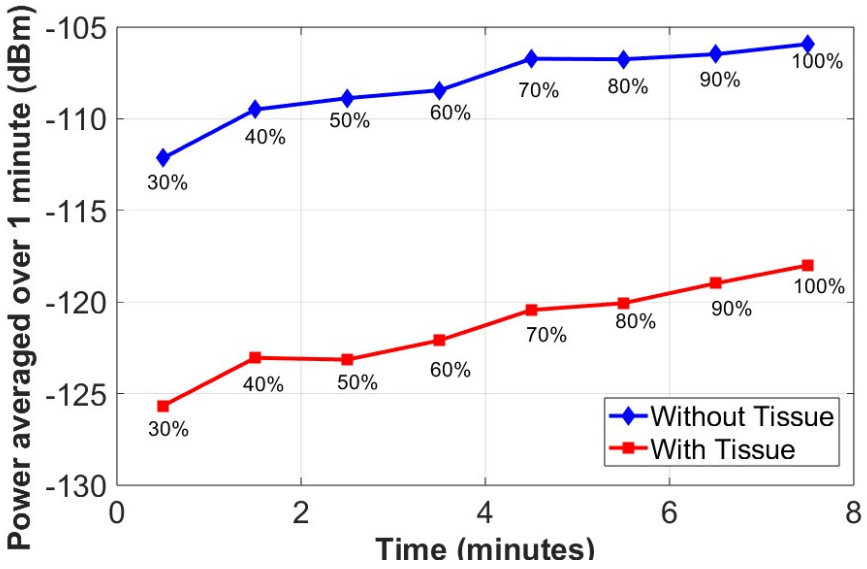

Figure 5.6: Received power at various logic utilization.

with and without a biological tissue. For the tissue simulations, we used a 4.5cm thick section of porcine tissue, comprising 0.7cm of skin, 1.3cm of fat, and 2.2cm of muscle. Figure 5.5 shows the experimental setup with tissue.

Figure 5.6 shows the received power averaged over 1 minute at different logic gate uti-

lization percentages for with and without tissue measurements. As can be observed from the plot, the received power from backscattering through tissue, is about 13dB lower than the received power from backscattering through air. Please note that the experimental setup used for Figure 5.4 has the transmitter at a distance of 13cm and the receiver at a distance of 13cm from the FPGA and in the case of Figure 5.6, the transmitter is at a distance of 13cm and the receiver was placed at a distance of 17cm from the FPGA. Hence there is a slight discrepancy in the received power values between both the cases.

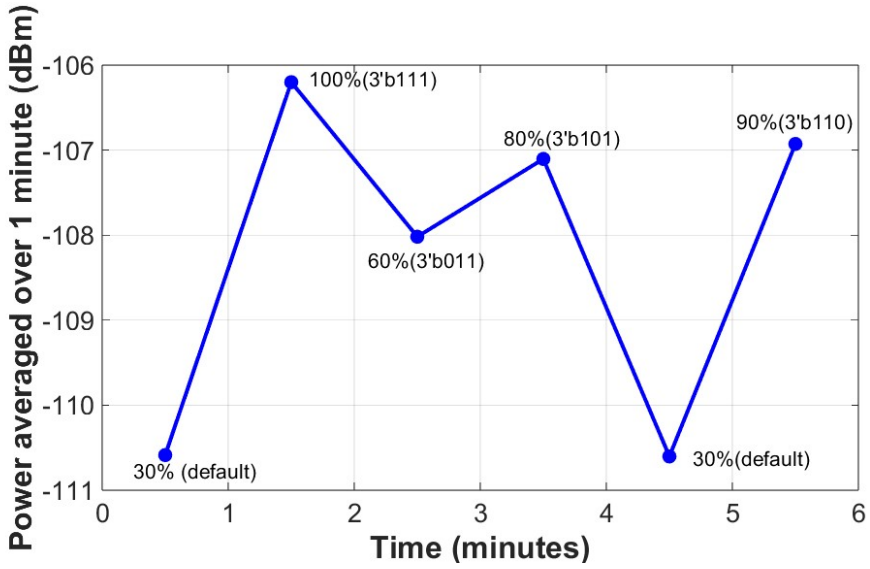

Figure 5.7: Received power at various logic utilizations controlled externally.

In the proposed system, a control signal requesting an increase in received power (i.e., higher logic utilization) is modulated into the carrier wave. After receiving and decoding this information at the control circuit of the tag, it is transmitted to the FPGA. Hence, we should be able to modify the logic gate utilization with an external control input. Please note, the primary focus of this work is on adaptively changing the amount of logic gate resources used for RFID backscattering based on a control input. We have conducted experiments to show that this system can actually modify the logic gate utilization with an external control input. This external control input is provided by programming the slide switches on the FPGA which can be used to input logic values '0' or '1'. We started with

the default setting at 3'b000, then switched it to 3'b111, 3'b011, 3'b101, 3'b000, 3'b110 for a 6 minute measurement recording. The notation 3'b011 represents a three-bit binary number. In this format, the '3' indicates the number of bits, 'b' stands for binary, and '011' is the binary value itself. The most significant bit (leftmost) is '0', and the least significant bit (rightmost) is '1'. Figure 5.7 shows the received power averaged over 1 minute for each of the logic utilization setting.

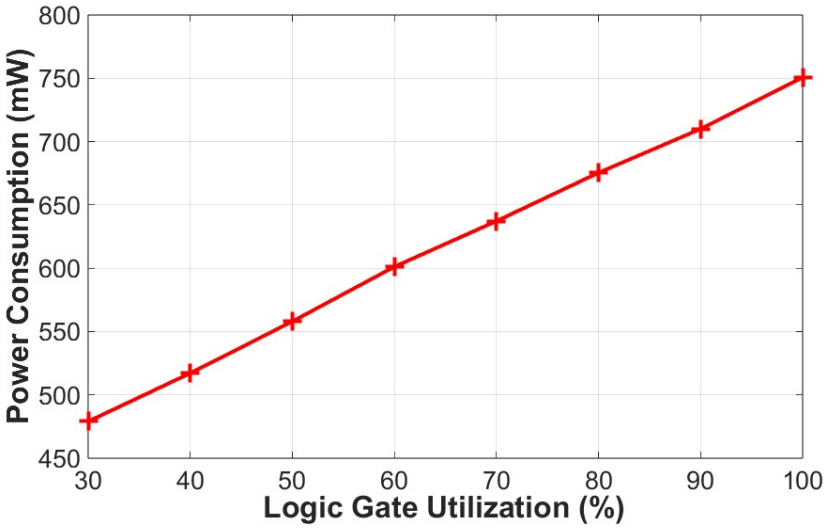

Figure 5.8: Power consumption by the FPGA.

Figure 5.8 presents the power consumption of the FPGA at different utilizations. It ranges from 479mW at 30% to 751mW at 100%. Although increased utilization leads to stronger signal reception, it also results in higher power consumption. In addition, the absolute power of about 0.48mW itself could be problematic for biomedical devices as these power values are excessive and could put a strain on its source. However, both of these power issues can be mitigated by switching to a low-power custom ASIC in future designs.

CHAPTER 6
CONCLUSION & DISCUSSION

This research builds on the work presented in [1], which explores the use of digital logic for backscattering communication in biotelemetry devices that can be implemented on an ASIC. It introduces an ASIC-based backscattering system that not only processes physiological data collected from various sensors within the body but also functions effectively as a biotelemetry device. This work proposed a key advancement which is the adaptive management of logic gate resources to enhance received power efficiency.

One of the challenges in the previous work was the need for manual adjustments of logic gate utilization using a programming software, compiling and reprogramming the device, a process that could take between 30 minutes to an hour. Moreover, once fabricated, such adjustments are too constraining in an ASIC. The system presented in this work allows for adaptive management of resources, significantly enhancing the device's functionality and flexibility in strength of the received power .

We have conducted successful measurements demonstrating that increased logic gate utilization directly correlates with enhanced received power. Results have been presented, from implementing an internal control logic that adjusts logic gate utilization by 10% every minute. In our experiments using an FPGA, we observed up to a 7dB enhancement in received power when logic gate utilization was increased from 30% to 100%. Furthermore, we have shown that these adjustments can be made without the need to re-program the FPGA. This system can greatly improve the operational efficiency. For example, in scenarios where the reader is not in close proximity to the tag, if the received power is low, the reader can request an increase in power from the tag.

Additionally, the use of external control logic to modify logic gate utilization adds further flexibility. Results have been provided for this case where control logic is provided using

the slide switches in the FPGA. In the case of an ASIC, this control input will be provided at the output of the tag's control circuit. This capability moves us closer to our ultimate goal of developing a system where logic gate utilization is dynamically adjusted based on the power received at the RFID reader. Future work will focus on creating a self-sufficient system where the reader can capture received information and modulate this data into the carrier wave, allowing the control input to be decoded and used to adjust the backscattering logic gate resources at the tag.

The advantages highlighted in previous work, such as frontend-less configuration, spectral flexibility, and versatility, still apply to our current work. However, the power consumption of the FPGA is high and could be problematic for use in biomedical devices. But, this problem can be rectified by implementing this design on a custom low-power ASIC for future design.

In conclusion, this work contributes to the design and development of an adaptive RFID ASIC backscattering system for biotelemetry applications.

REFERENCES

[1] S. Sangodoyin, E. M. Ugurlu, M. Dey, M. Prvulovic, and A. Zajić, "Leveraging on-chip transistor switching for communication and sensing in neural implants and gastrointestinal devices," *IEEE Transactions on Biomedical Engineering*, vol. 69, no. 1, pp. 377–389, 2021.

[2] C.-L. Cheng, L. N. Nguyen, M. Prvulovic, and A. Zajić, "Exploiting switching of transistors in digital electronics for rfid tag design," *IEEE Journal of Radio Frequency Identification*, vol. 3, no. 2, pp. 67–76, 2019.

[3] S. A. Weis, "Rfid (radio frequency identification): Principles and applications," *System*, vol. 2, no. 3, pp. 1–23, 2007.

[4] F. Nekoogar and F. Dowla, *Ultra-wideband radio frequency identification systems*. Springer Science & Business Media, 2011.

[5] T. Inaba, "Value of sparse rfid traceability information in asset tracking during migration period," in *2008 IEEE International Conference on RFID*, IEEE, 2008, pp. 183–190.

[6] M. Baghaei-Nejad *et al.*, "A remote-powered rfid tag with 10mb/s uwb uplink and-18.5 dbm sensitivity uhf downlink in 0.18 μm cmos," in *2009 IEEE International Solid-State Circuits Conference-Digest of Technical Papers*, IEEE, 2009, pp. 198–199.

[7] A. Lazaro, A. Ramos, R. Villarino, and D. Girbau, "Active uwb reflector for rfid and wireless sensor networks," *IEEE transactions on antennas and propagation*, vol. 61, no. 9, pp. 4767–4774, 2013.

[8] A. Ranganathan, B. Danev, and S. Capkun, "Proximity verification for contactless access control and authentication systems," in *Proceedings of the 31st Annual Computer Security Applications Conference*, 2015, pp. 271–280.

[9] "Cequr simplicity - simplifying insulin management." Accessed: 2024-04-10. (Access month 2024).

[10] N. F. Rinsma, N. D. Bouvy, A. A. Masclee, and J. M. Conchillo, "Electrical stimulation therapy for gastroesophageal reflux disease," *Journal of neurogastroenterology and motility*, vol. 20, no. 3, p. 287, 2014.

[11] Unknown. "Ingestible thermometer pill aids athletes in beating the heat." (2010), (visited on 04/10/2024).

[12] T. S. Rappaport, A. Annamalai, R. M. Buehrer, and W. H. Tranter, "Wireless communications: Past events and a future perspective," *IEEE communications Magazine*, vol. 40, no. 5, pp. 148–161, 2002.

[13] K. S. Nikita, *Handbook of biomedical telemetry*. John Wiley & Sons, 2014.

[14] C. Byrne and C. L. Lim, "The ingestible telemetric body core temperature sensor: A review of validity and exercise applications," *British journal of sports medicine*, vol. 41, no. 3, pp. 126–133, 2007.

[15] S. Zhang *et al.*, "A ph-responsive supramolecular polymer gel as an enteric elastomer for use in gastric devices," *Nature materials*, vol. 14, no. 10, pp. 1065–1071, 2015.

[16] G. Fuhrmann *et al.*, "Sustained gastrointestinal activity of dendronized polymer–enzyme conjugates," *Nature chemistry*, vol. 5, no. 7, pp. 582–589, 2013.

[17] B. Laulicht, N. J. Gidmark, A. Tripathi, and E. Mathiowitz, "Localization of magnetic pills," *Proceedings of the National Academy of Sciences*, vol. 108, no. 6, pp. 2252–2257, 2011.

[18] Z. Xiao *et al.*, "An implantable rfid sensor tag toward continuous glucose monitoring," *IEEE journal of biomedical and health informatics*, vol. 19, no. 3, pp. 910–919, 2015.

[19] H. Jiang, X. Zhou, S. Kulkarni, M. Uranian, R. Seenivasan, and D. A. Hall, "A sub-1 μw multiparameter injectable biomote for continuous alcohol monitoring," in *2018 IEEE Custom Integrated Circuits Conference (CICC)*, IEEE, 2018, pp. 1–4.

[20] W. Jeon, J. Melngailis, and R. W. Newcomb, "Disposable cmos passive rfid transponder for patient monitoring," in *2006 IEEE International Symposium on Circuits and Systems (ISCAS)*, IEEE, 2006, 4–pp.

[21] H. Cao *et al.*, "An implantable, batteryless, and wireless capsule with integrated impedance and ph sensors for gastroesophageal reflux monitoring," *IEEE Transactions on Biomedical Engineering*, vol. 59, no. 11, pp. 3131–3139, 2012.

[22] A. Kiourti, C. W. Lee, J. Chae, and J. L. Volakis, "A wireless fully passive neural recording device for unobtrusive neuropotential monitoring," *IEEE Transactions on Biomedical Engineering*, vol. 63, no. 1, pp. 131–137, 2015.

[23] H. N. Schwerdt, F. A. Miranda, and J. Chae, "Wireless fully passive multichannel recording of neuropotentials using photo-activated rf backscattering methods," *IEEE Transactions on Microwave Theory and Techniques*, vol. 63, no. 9, pp. 2965–2970, 2015.

[24] D. Vasisht, G. Zhang, O. Abari, H.-M. Lu, J. Flanz, and D. Katabi, "In-body backscatter communication and localization," in *Proceedings of the 2018 Conference of the ACM Special Interest Group on Data Communication*, 2018, pp. 132–146.

[25] A. Aberra, Y.-H. Kim, M. Je, and S. Ha, "Backscatter communication for biomedical devices," in *Handbook of Biochips: Integrated Circuits and Systems for Biology and Medicine*, Springer, 2022, pp. 745–762.